CAV2021
11th International Symposium on Cavitation
May 10-13, 2021, Daejon, Korea

Detachment of Cavitating Rings in a Long-throat Venturi Tube

Javier Rosas[1], Jorge Naude[2], Federico Méndez[2], Rodrigo Mayén[3] and Margarita Navarrete[1*]

[1]Instituto de Ingeniería, PUNTA-UNAM, Apodaca, Nuevo León 66629, México
[2]Departamento de Termofluidos, Facultad de Ingeniería, UNAM, CdMx 04510, México
[3]Facultad de Química, PUNTA-UNAM, Apodaca Nuevo León 66629, México

Abstract: We analyze cavitation dynamics, instabilities and detachment mechanism in an axisymmetric long throat Venturi tube. Experimental runs were carried out to study the stages from no cavitating to choked-flow conditions (water). Based on this experimental data, a numerical study using an incompressible cavitation phase–change solver is performed to simulate the dynamics involved in the transition from sheet cavitation to periodically shedding of large vapor cloud separated from the apex cavitation ring advected downstream. Numerical simulations are performed considering a three-dimensional, axisymmetric model using a commercial CFD package. The evolution of experimental and computed pressure is shown in plots 2D-3D.

Keywords: Cavitating venturi; two phase flow; choked flow; high performance computing.

1. Introduction

The behavior of cavitating Venturi nozzles has been broadly investigated over the past 65 years because of the wide range of phenomena associated with their flow [1]. Cavitating Venturi nozzles in choked conditions are known to be used for mass flow control. Under such condition, the pressure within the throat reaches the liquid saturation pressure, so the mass flow rate remains constant [2]. Its complex behavior is characterized by instabilities, during which transient cavities shed downstream. Two regions drive its cavitation pattern: cavity detachment and cavity closure. The shedding vapor clouds have different origins: either the cloud is generated by vortex shedding filled with bubbles or produced by periodic pressure disturbances by the average flow.

A theoretical development for bubble flows can be found in [2]. It presents as well experimental measurements that emphasizing the role of the void fraction. The work in [3] lays the same line of research, but including a theoretical-experimental treatment of shock emissions. The authors in [4], provide a robust set of expressions for the flow and shock waves generated within the nozzle. The design of commercial Venturi flow meters/controllers by ASME standards is a topic of great importance [5], as the flow behavior depends on the Venturi geometry, pressure ratio, mixture velocity, water aeration, etc.. Numerical studies have been conducted to find the optimal geometry for cavitation activity and periodic cavitation shedding in a Venturi [6-8]. The numerical codes however do not take into account the formation of complex flow patterns that may affect the proper operation and/or calibration of the device. The numerical study in the present work emulate the experimental observations of the flow dynamics produced in a long-throat Venturi. The data, geometry and conditions of our experimental rig are used to feed the model.

2. Materials and Methods

A hydraulic circuit is designed, manufactured, and set up to characterize the dynamic behavior of cavitation devices. A complete description of the system is found in reference [9]. The main components and instrumentation are a 5 hp centrifugal pump with variable frequency driver, a 70 l water tank with

* Corresponding Author: Margarita Navarrete, mnm@pumas.iingen.unam.mx

temperature control, manual ball valves, an auxiliary tank, an acrylic Venturi tube (see Figure 1), a flowmeter, and a Phantom v9.1 camera to record video at rates ranging from 25000 to 40000 fps.

..

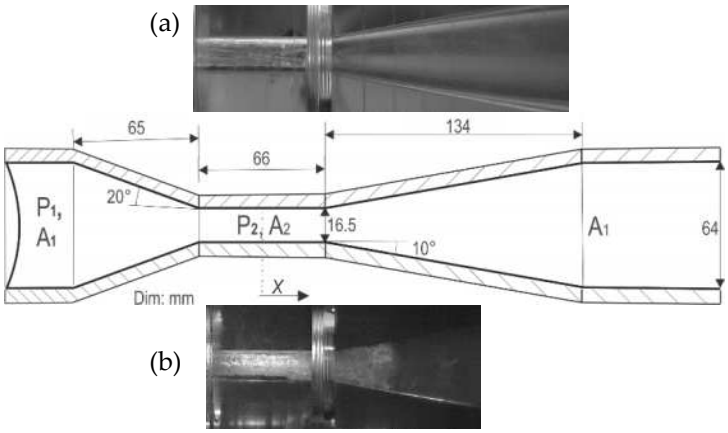

Figure 1. Schematic view of the Venturi profile with dimensions, were L is the throat length, D is the inlet and outlet diameter and P_1, P_2 are the inlet and throat pressure, respectively. The throat section has an L/D ratio equal to 4, assuring that all nuclei grow to a detectable size (by human eye and cameras), its long path guarantees heat transfer and visualization of the flashing vaporization process, as seen in images (a) and (b).

2.1 Numerical model

We choose to emulate the cycle that sustains the choked flow condition within the long throat Venturi, until the cavitating ring detaches. This condition is reached experimentally when the tap-water flow-rate at the venturi inlet is set at 1.12 ms^{-1}. The initial vapor fraction is fixed at of 0.001 and room temperature.

The Reynolds averaged equations (RANS) approximation is applied. To simulate cavitation, a mass transfer model proposed by Schnerr and Sauer is included, as well as turbulence using the k-ε RNG model. For the pressure-velocity coupling, PISO and PRESTO schemes are chosen. The Mixture model to solve the two-phase flow is applied. With regard to density, turbulent kinetic energy, and turbulent dissipation a second-order spatial discretization scheme is used. The outlet relative pressure is set at 0 Pa to fix the flow direction, and the liquid temperature is set to 300 K. The detachment of the cavitating rings in the long-throat Venturi tube is studied as a function of time under the aforementioned conditions. A time step is calculated from the Courant number, 10 μs, and time zero is set when the minimum vapor length in throat occurs. The numerical results are considered valid when simulation reaches the stable condition.

3. Results

3.1 Experimental

Tap water at room temperature is pumped in saturated conditions, the liquid circulates by fifteen minutes. The pump power afterwards increased in steps of 1% or 5% until the choking flow condition is reached, as observed in the behavior profiles of the cavitation number and P_2/P_1 ratio, shown as a function of pump power, in Figure 2a (cavitation number and P_2/P_1 ratio as a function of pump power). The curves clearly show the initial liquid-vapor phase change, and the pressure ratio oscillations to achieve a constant flow rate. From the experimental runs and the analysis of the recorded video, as well as the flow parameters, we find the following stages:

a) *Fluctuation in venturi throat*. Many cycles of flashing vaporization and condensation are needed to achieve the length and thickness of the cavity around the cylindrical long throat, until sheet cavitation is

* Corresponding Author: Margarita Navarrete, mnm@pumas.iingen.unam.mx

established, the cavity does not appear instantly at 2/3 of the throat as some authors claim. The cyclic process starts at a low frequency (appear /disappear and move on over a small liquid layer attached on the walls), but when the sheet reaches the middle of throat the process is accelerated.

b) *Shedding*. When the sheet cavity reaches almost the throat- diffuser intersection, it joins with a weak cavitating ring that has formed previously in this interface. Later on, the closure of the sheet cavity and a stagnation point are generated. The conservation of momentum causes the liquid to enter below the cavity (re-entrant jet) and the separation of vapor as a ring-shaped cloud occurs. It is advected downstream, where it eventually collapses. Under certain conditions, the cyclic collapsing produces shock waves that expands both upstream and downstream, and when the wave reaches the throat zone all vapor structures condense. When the sheet cavitation and ring-shaped cloud regenerate cyclically, the choked flow condition is established. Under this condition a numerical simulation will be developed to emulate the cycle which sustains the choked flow.

3.2 Numerical simulation of the cycle which sustains the choked flow within Venturi tube

Figure 2b shows the pressure evolution at the middle Venturi tube section as a function of time. The cycle begins when the pressure drops and extends up to near 2/3 of the throat, forming a vapor ring around its wall with a thickness of about 1.14 mm (Figure 2, t= 0 ms, and Figure 3, frame 1). Vapor is genrated as well at the interface (Figure 3, frame 2). As the pressure continues to drop (Figure 2b, t= 6 ms), both cavities merge (Figure 3, frame 5). The cavity continues to grow and detaches downstream as a cavitating ring (Figure 3, frames 7-11). This detachment is caused by liquid recirculation on the borders of the diffuser. The cavitating ring is shifted by this pressure wave (Figure 2, indicated by arrows in profiles t= 8, t= 10 and t= 13,). When the pressure wave dampens by the hydrostatic pressure, it causes ring condensation (Figure 3, frame 17).

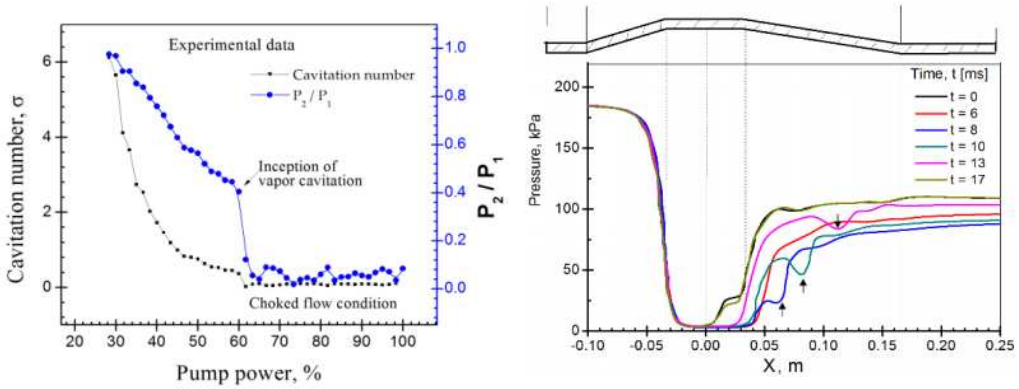

Figure 2. (a) Experimental data, profiles of cavitation number, and P_2/P_1 ratio as a function of the % of pump power. (b) Numerical profiles of the pressure as a function of time and location. The profiles show the shift of a pressure wave (that drags the cavitating ring) until it disappears downstream. The pressure fluctuation is indicated by arrows in profiles t=8, t=10 and t= 13 ms).

4. Conclusions

The numerical (within CFD framework) and experimental studies performed in the present work allowed some of the fluid-flow events occurring within a long-throat cavitating venturi, under choke conditions. The main results are summarized as follows: (1) the evolution of cavitation can be divided in the following stages: inception, development (sheet cavitation), detachment (separation between cavity and the wall), shedding (acceleration of the cloud ring towards downstream), collapse and rebound. The

* Corresponding Author: Margarita Navarrete, mnm@pumas.iingen.unam.mx

inception is characterized by many flashing vaporization-condensation cycles before reaching the length and thickness necessary around the long throat, in which sheet cavitation is established; meanwhile, at the throat-diffuser interface a new cavity is generated. Two different paths can be identified here: collapse or merge with the sheet cavity. For both of them, the attached cavity grows downstream, meanwhile, the previous cloud ring cavity is collapsing. The frequency of such experimentally-observed evolution cycle (from inception to collapse and rebound) varies as a function of time due to changes in temperature. The numerical simulation of the ring cloud shedding cycle (from sheet cavitation to collapse) covered only the mechanism induced by re-entrant jet and pressure waves. Our future research will focus on the study of the coalescence and fragmentation of the detached cavity.

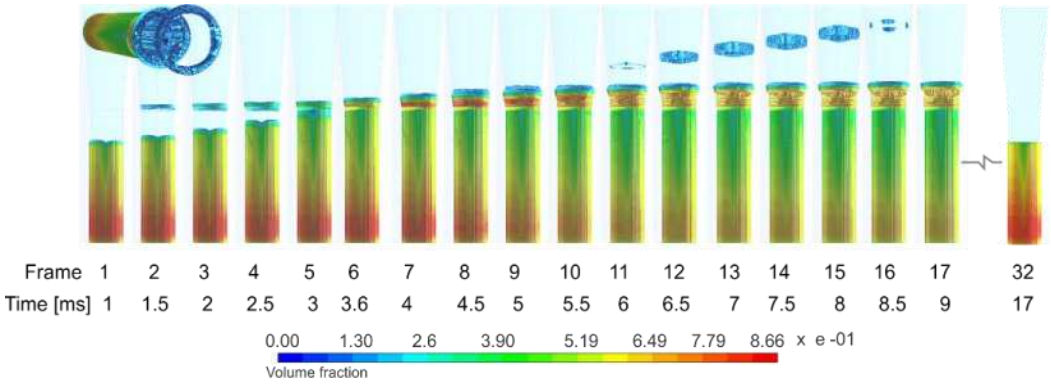

Figure 3. Numerical results from the temporal evolution of the cavity shedding cycle. Isosurfaces of the vapor as a funtion of time. The frequency shedding is about 58.8 Hz, pressure ratio ~ 0.016, and Reynols number ≅ 70000. A complementary video for the experimental and the numerical part in: https://drive.google.com/drive/folders/1HZCAkjFnMpCJlVs7GFplpGMi5ktRDqi3?usp=sharing

Acknowledgments: This work has supported by the Dirección General de Asuntos del Personal Académico, Universidad National Autónoma de Mexico, UNAM, under the research grant PAPIIT - IN106919.

References

1. Jarman, P.; Taylor, K. Light flashes and shocks from a cavitating flow, *Brit. J. Appl. Phys*., **1965**, *16*, 675-683.
2. Ishii, R.; Yoshikuni, U.; Shigeaki, M.; Norihiki, S. Bubbly flows through a converging-diverging nozzle, *Phys. Fluids A: Fluid. Dyn*. **1993**, *5*, 1630-1643.
3. Ando, K.; Sanada, T.; Inaba, K.; Damazo, J.; Shepherd, J.; Colonius, T.; Brennen, C.E. Shock propagation through a bubbly liquid in a deformable tube, *J. Fluid Mech*. **2011**, *671*, 339-363.
4. Pasinlioglu, S.; Delale, C.F.; Schnerr, G.H. On temporal stability of steady-state quasi- 1D bubbly cavitating nozzle flow solutions, *IMA J. of Appl. Math*., **2009**, *74*, 230-249.
5. Measurement of gas flow by means of critical flow Venturi nozzles, *ASME MFC-7M*, **1987**.
6. Kuldeep; Saharan, V.K. Computational study of different Venturi and orifice type hydrodynamic cavitating devices. *Journal of Hydrodynamics*, **2016**, *28(2)*, 293–305.
7. Charrière, B.; Goncalves, E. Numerical investigation of periodic cavitation shedding in a Venturi. *International Journal of Heat and Fluid Flow*, **2017**, *64*, 41–54.
8. Fang, L.; Wei, L.; Li, Q.; Wang, Z. Numerical investigation of the cavity shedding mechanism in a Venturi reactor, *International Journal of Heat and Mass Transfer*, **2020**, 156, 119835.
9. Navarrete, M.; Naude, J.; Méndez, F.; Godínez, F.A. Dynamics and acoustics of a cavitating Venturi flow using a homogeneous air-propylene glycol mixture, *Proceedings of the 9th International Symposium on Cavitation (CAV2015) Journal of Physics: Conference Series* 656, **2015**, 012103.

* Corresponding Author: Margarita Navarrete, mnm@pumas.iingen.unam.mx